

Electrosynthesis of Cu₅Zn₈ Alloy in Zinc Oxide-urea/ 1-ethyl-3-methylimidazolium Fluoride System at 353 K

Wencai He¹, Peng Chen¹, Wentao Deng¹, Zhongning Shi^{1,*}, Bingliang Gao¹, Xianwei Hu¹, Junli Xu², Zhaowen Wang¹

¹ School of Metallurgy, Northeastern University, Shenyang 110819, China

² College of Sciences, Northeastern University, Shenyang 110819, China

*E-mail: znshi@mail.neu.edu.cn

Received: 19 November 2016 / Accepted: 24 December 2016 / Published: 30 December 2016

To solve problems of conventional methods in which the high temperatures, extreme pressures and huge currents are used in preparation process of Cu₅Zn₈ alloy, it's necessary to develop low-temperature and low-energy technology. In this study, a low temperature (353 K) electrodeposition method for preparation of Cu₅Zn₈ alloy was proposed. A new electrolyte used in this study, urea/ 1-ethyl-3-methylimidazolium fluoride, can surprisingly dissolve zinc oxides. ZnO was chosen as a zinc source instead of ZnCl₂ used in the conventional method. A Cu cathode was employed as the copper source in situ operation instead of the conventional method that copper source is introduced by adding copper salts. The electrochemical behavior of zinc in the system was investigated using linear sweep voltammograms and cyclic voltammetric techniques. The results illustrated that the zinc reduction is a diffusion-controlled irreversible process via a single-step two-electron transfer procedure. The diffusion coefficient was $1.8 \times 10^{-8} \text{ cm}^2 \text{ s}^{-1}$. Electrode reaction becomes more reversible and equal potentials shift toward the positive direction as temperature increases from 333 to 373 K. Electrodeposition experiments are performed on a Cu cathode and electrodeposits are identified as Cu₅Zn₈ alloy via XRD and EDS. The cross-sectional SEM showed that a distinguishable layer of Cu₅Zn₈ alloy was discovered on the surface of the Cu cathode and the thickness of this Cu₅Zn₈ layer was approximately 2 μm . An EDS linear scanning analysis for this layer showed that a high concentration of zinc atoms was distributed on the surface and the copper atoms were mainly concentrated at the bottom of the Cu cathode. A possible formation mechanism for Cu₅Zn₈ alloy was proposed.

Keywords: Cu₅Zn₈; 1-ethyl-3-methylimidazolium fluoride; zinc oxide; γ -brass; Ionic liquid

1. INTRODUCTION

Copper tubes are widely applied for condensers in oil refineries. Cu₅Zn₈, γ -brass, is a special Cu-Zn alloy that has often been used as a Hume-Rothery phase material and additive in oil-based

fluids to improve thermal conductivity [1-2]. If Copper tubes are coated with Cu_5Zn_8 layer, the cooling rapid for oil will be improved. Traditionally, Cu_5Zn_8 has been prepared via wire electrical explosion [3], electric arc discharge [4] or mechanical alloying/milling [5]. Wang employed the wire electrical explosion method to prepare Cu_5Zn_8 , in which the shape of most particles was hexagonal and the size complied with the log-normal distribution law [3]. Farbod [2, 4] used the electric arc discharge method to generate Cu_5Zn_8 particles and studied the effect of sintering temperature on the physical properties of Cu_5Zn_8 and the relationship between Cu_5Zn_8 and the thermal conductivity of oil-based fluids. The Mukhopadhyay group fabricated Cu_5Zn_8 using mechanical milling/alloying and studied the evolution of its structures and phases [5]. However, these methods all require high temperatures, extreme pressures and huge currents. For example, in the wire electrical explosion method, a high voltage (3.6×10^4 V) is employed to discharge pulse current [3]. The electric arc discharge method is performed at 400 A and 3 atm [4]. And mechanical alloying/milling involves melting at a high temperature of 1243 K [5]. Therefore, it's necessary to develop low-temperature and low-energy technology for preparation of Cu_5Zn_8 alloy. In this study, we attempted to electroplate Cu_5Zn_8 alloy on a Cu substrate in room temperature ionic liquids (RTILs) at a relative mild condition (353 K, -2.05 V and normal atmospheric pressure).

In recent years, RTILs have been used as electrolytes in the electrochemical processes [6-14]. Some RTILs have been used to electrodeposit Cu_5Zn_8 . For example, a ZnCl_2 -[EMI][Tf₂N] ionic liquid was used to prepare Cu_5Zn_8 via a reduction-diffusion method in two separate baths [15]. A ZnCl_2 -EMIC ionic liquid has been employed to electrodeposit copper-zinc alloys and Cu_5Zn_8 was observed after these alloys were being dealloyed at 0.1 V [16]. For these ionic liquids, ZnCl_2 was used as a zinc source. However, ZnCl_2 is vulnerable to hydrolysis and is extremely toxic to humans [22]. Therefore, we choose ZnO as a zinc source instead of ZnCl_2 because it is more eco-friendly and omits steps related to prechlorination. However, most metal oxides are not soluble in molecular solvents, except for aqueous acids or alkalis. Interestingly, in this study, a new electrolyte which is insensitive to water and stable in air, urea /1-ethyl-3-methylimidazolium fluoride (urea/EMIF), is able to selectively dissolve zinc oxides. Moreover, we select a Cu cathode as the copper source instead of the conventional method that copper source is introduced by adding copper salts. Therefore, ZnO-urea/EMIF is a potential electrolyte for preparation of a copper tube which has a good thermal conductivity for oil-based fluids.

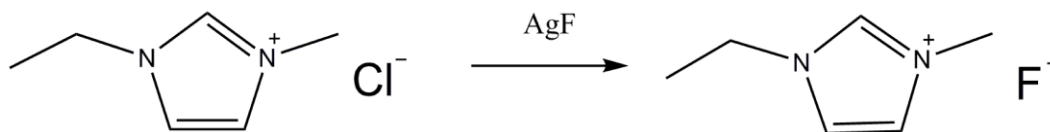
In this work, we electrochemically prepared Cu_5Zn_8 alloy on a Cu cathode in a ZnO-urea/EMIF system at 353 K. We investigated the electrochemical behavior of zinc in this system using linear sweep voltammograms (LSV) and cyclic voltammograms (CV). We also carried out potentiostatic experiments on a copper cathode and the electrodeposits were characterized via X-ray diffraction (XRD), energy dispersive spectroscopy (EDS) and scanning electron microscope (SEM). A possible formation mechanism for Cu_5Zn_8 was proposed.

2. EXPERIMENTAL

The raw materials of EMIC ($\text{C}_6\text{H}_{11}\text{N}_2\text{Cl}$, >98%) purchased from the Lanzhou Institute of Chemical Physics China was purified according to the procedure described in the literatures [17-18].

Urea and ZnO were purchased and dried following the method reported in the literature [19]. Analytic grade reagent AgF (>98%) purchased from Alfa Aesa and was used as received.

EMIF was prepared by reacting EMIC with AgF through a double replacement reaction, as shown in Scheme 1.



Scheme 1. Synthesis of EMIF by reacting EMIC with AgF.

EMIC was mixed with AgF (1:1 molar ratio) in a solution and stirred continuously for 2 h. AgCl was precipitated immediately on the bottom. A titration and back titration process was performed until no AgCl precipitation generated on the bottom of the solution. AgCl was removed from the mixed solution by a funnel and centrifuge contactor. The filtrate was distilled in a rotary evaporator to remove water and dried using a high-powered vacuum pump. The purified EMIF was obtained from the filtrate.

Urea and EMIF (molar ratio=2:1) was mixed in the argon-filled glove box at 353 K. 3 mmol ZnO was added into the mixture and stirred continuously until ZnO was completely dissolved. Thus, an electrolyte (ZnO-urea/EMIF) was obtained.

The electrochemical behavior of the ZnO-urea/EMIF system was recorded by LSV, CV and potentiostatic techniques using a potentiostat and galvanostat in an electrochemical cell that was described in a previous literature [19]. A W, Pt, Ag wire (99.95%) was used as the working electrode, counter electrode and quasi-reference electrode, respectively. All electrodes are polished with emery paper, cleaned with ultrasonic waves in an alcohol solution. To electrosynthesize Cu₅Zn₈ alloy, potentiostatic experiments are performed on a copper cathode (0.55 cm², 99.99%). Cu cathode was used as a copper source for Cu₅Zn₈ alloy. After potentiostatic electrodeposition experiments, electrodeposits were obtained on the surface of Cu cathode.

Phase constitution and morphology of electrodeposits was detected via XRD (PANalytical MPDDY 2094, the Netherlands) and a SEM machine (ZEISS ULTRA-43-13, Germany) equipped with an EDS (X-Max 50, Oxford).

3. RESULTS AND DISCUSSION

3.1 Cyclic voltammetry and linear sweep voltammetry

To study the electrochemical behavior of zinc in the ZnO-urea/EMIF system, CV was recorded using a copper working electrode at 353 K. The CV scan started from 1.4 V (vs. Ag) to the first vertex of -2.2 V, and then reversed to 1.4 V, as illustrated in Figure 1. It is clear that a cathodic peak can be observed at around -1.88 V, whereas an anodic peak is presented at approximately 0.87 V. The

cathodic peak was assigned as the reduction of Zn (II) to Zn (0), indicating that the electrodeposition of Zn occurs through a single-step two-electron transfer procedure [19]. Correspondingly, the anodic peak was recognized as the anodic stripping of Zn electrodeposited in the previous negative sweep [19].

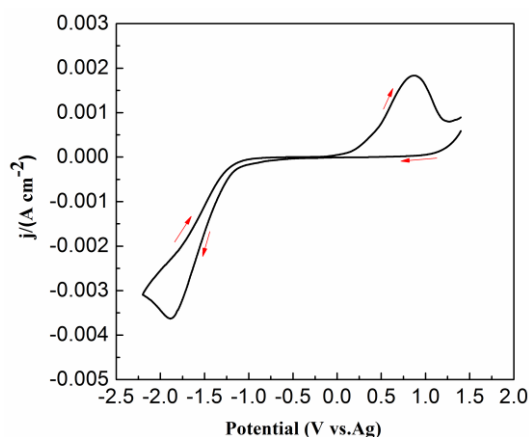


Figure 1. Cyclic voltammograms of the Urea/EMIF (2:1 molar ratio) containing 3 mmol ZnO using a copper working electrode at 353 K. The scan rate was $0.05 \text{ V} \cdot \text{s}^{-1}$.

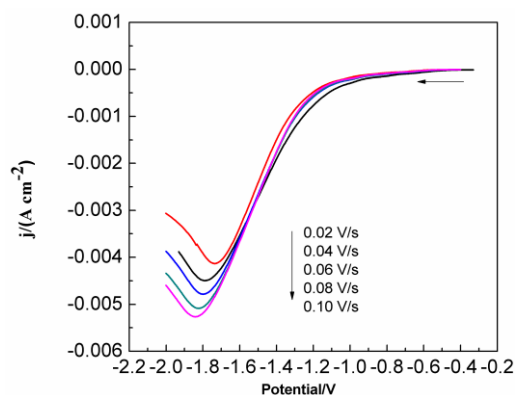


Figure 2. Linear sweep voltammograms of the urea/EMIF (2:1 molar ratio) containing 3 mmol ZnO using a copper working electrode under different scan rates at 353 K.

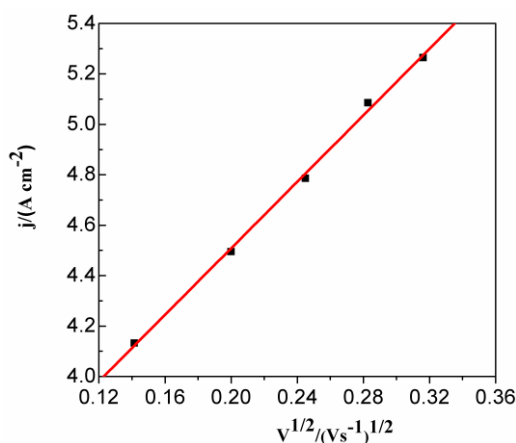


Figure 3. The cathodic peak current density as a function of the square root of scan rates using a copper working electrode in the urea/EMIF (2:1 molar ratio) containing 3 mmol ZnO at 353 K.

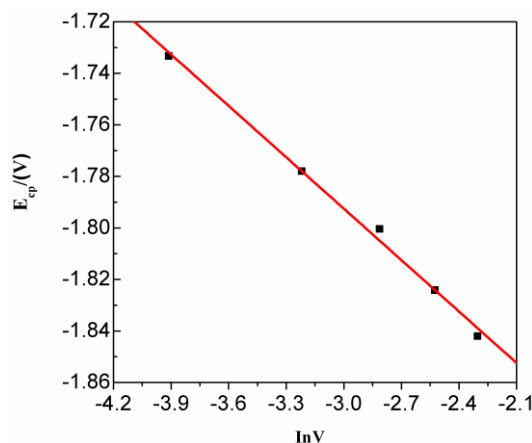


Figure 4. The cathodic peak potentials as a function of the scan rates ($\ln v$) using a copper working electrode in the urea/EMIF (2:1 molar ratio) containing 3 mmol ZnO at 353 K.

LSV under different scan rates are shown in Figure 2. The cathodic peak potential (E_{cp}) shifts to the negative direction and the cathodic peak current density (j_p) rises slowly as increase of scan rates. For further study, the correlation of j_p obtained from Figure 2 against scan rates are presented in Figure 3. A linear correlation between j_p and $v^{1/2}$ was obtained. Accordingly, cathodic peak potentials also increase with increasing scan rates. An approximately linear correlation between cathodic peak potentials and scan rates is presented in Figure 4. Values of difference between E_{cp} and the cathodic half-peak potential ($E_{cp/2}$) under different scan rates are listed in Table 1.

Table 1. Comparisons of the difference between the cathodic peak potential and the cathodic half-peak potential in Figure 2 under different scan rates.

$v/v \text{ s}^{-1}$	$ E_{cp}-E_{cp/2} /mV$
0.02	269.7
0.04	349.1
0.06	327.3
0.08	339.2
0.10	349.1

The difference for $|E_{cp}-E_{cp/2}|$ is increased as the increasing of scan rates. At the lowest scan rate, the value for $|E_{cp}-E_{cp/2}|$ is 269.7 mV, which is larger than that for a reversible process (33.5 mV at 353 K). All these characteristics suggest that the reduction of zinc in the ZnO-urea/EMIF system is a diffusion-controlled irreversible process and proceeds via a single-step two-electron transfer procedure [23-24].

For an irreversible charge transfer process, the transfer coefficient α can be obtained from the following equation [23].

$$|E_{cp} - E_{cp/2}| = 1.857RT/\alpha nF \quad (1)$$

Where E_{cp} is the cathodic peak potential in V, $E_{cp/2}$ is the cathodic half-peak potential in V, R is the gas constant $8.314\text{J}\cdot\text{K}^{-1}\text{mol}^{-1}$, T is the absolute temperature in K, α is the transfer coefficient, n_α is

the number of exchanged electrons, F is the Faraday constant $96485\text{C}\cdot\text{mol}^{-1}$. The values for $|E_{cp}-E_{cp/2}|$ under different scan rates can be obtained in Table 1.

For an irreversible reaction, the diffusion coefficient of Zn (II) species could be calculated according to the following equation [23].

$$j_p = 0.4958nFAc^0(\alpha n_\alpha F/RT)^{1/2}D^{1/2}\nu^{1/2} \quad (2)$$

Where j_p is the cathodic peak current density in A cm^{-2} , n_α is the number of exchanged electrons, A is the electrode area in cm^2 , c^0 is the initial concentration in $\text{mol}\cdot\text{cm}^{-3}$, D is the diffusion coefficient in cm^2s^{-1} , ν is the scan rate in $\text{V}\cdot\text{s}^{-1}$, and all other symbols have the same definitions as in the previous equation. The slope of the linear dependence of the j_p on $\nu^{1/2}$ was shown in Figure 3.

Introduction of the Eq. (1) into (2) yields a value of the diffusion coefficient D of Zn (II) in the ZnO-urea/EMIF system at 353 K ($7.4\times 10^{-10}\text{cm}^2\text{s}^{-1}$).

In addition, a summary for zinc diffusion coefficients in various ionic liquids is showed in Table 2. The difference for zinc diffusion coefficient in various ionic liquids may be related to different temperatures and various electrolytes systems.

Table 2. Summarization for zinc diffusion coefficients (D) in various ionic liquids.

Ionic liquid	Temperature (K)	D (cm^2s^{-1})	Reference
Urea/EMIF	353	7.4×10^{-10}	This work
Urea/ChCl	363	7.8×10^{-9}	[25]
AlCl_3 -MeEtimCl	313	6.7×10^{-7}	[26]

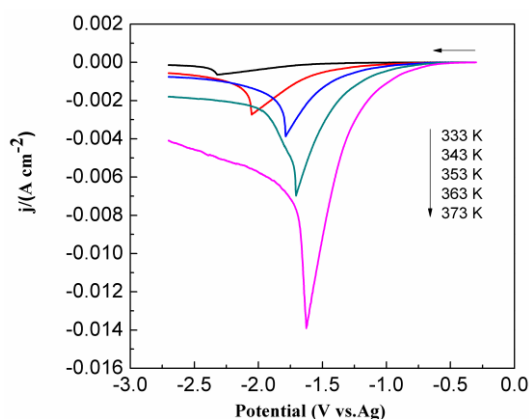


Figure 5. Linear sweep voltammograms of the urea/EMIF (2:1 molar ratio) containing 3 mmol ZnO using a copper working electrode at different temperature

Figure 5 shows the effect of temperature on LSV in the ZnO-urea/EMIF system. As temperature increases from 333 to 373 K, the cathodic peak potential anodically shifts. The difference between the cathodic peak potential and the cathodic half-peak potentials narrows (see Table 3). This means that electrode reaction becomes more reversible as the increment of temperatures. Moreover, equal potentials in LSV shift toward the positive direction, as shown in Figure 6. Similarly, the cathodic peak currents also increase with increasing temperature.

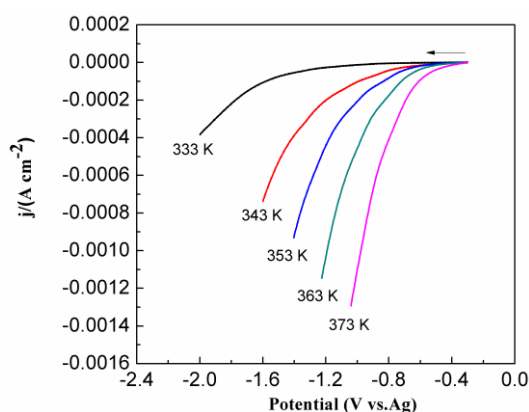


Figure 6. The equal potentials for the urea/EMIF (2:1 molar ratio) containing 3 mmol ZnO using a copper working electrode at various temperatures.

Table 3. Comparisons of the difference between the cathodic peak potential and the cathodic half-peak potential in Figure 5 under different temperatures.

Temperature/K	$ E_{cp} - E_{cp/2} / mV$
333	388.2
343	275.9
353	193.0
363	190.4
373	190.1

This is likely related to the enhancement of species diffusion at a higher temperature. Cathodic peaks become sharper with increasing temperatures due to the rapid decrease of zinc species concentration in the negative sweep.

3.2 Formation of Cu_5Zn_8 alloy

To prepare Cu_5Zn_8 alloy, potentiostatic experiments are performed on a Cu cathode and the relationship between current density and time during the potentiostatic electrodeposition was recorded in Figure 7. The current density sharply decreases at the beginning and remains relatively steady over the rest of the experimental period. Electrodeposits are obtained on the Cu cathode after potentiostatic experiments.

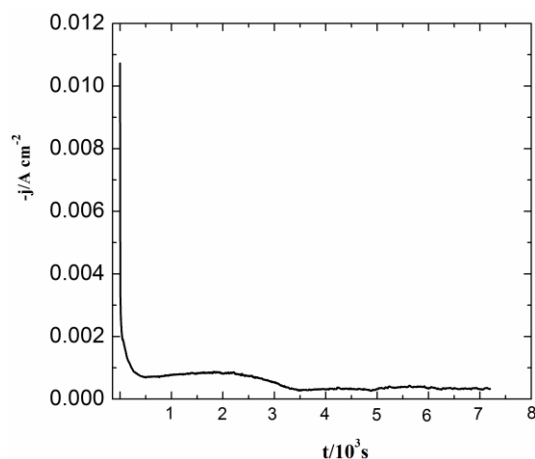


Figure 7. Current density as a function of the time for potentiostatic electrodeposition in the Urea/EMIF (2:1 molar ratio) containing 3 mmol ZnO on a copper cathode at -2.05 V.

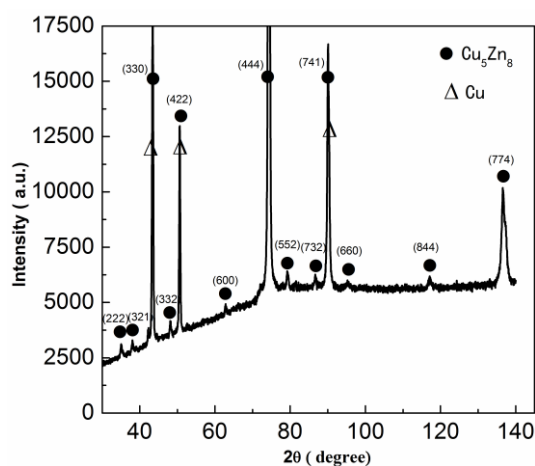


Figure 8. XRD pattern of electrodeposits obtained at -2.05 V on a Cu cathode in the urea/EMIF (2:1 molar ratio) containing 3 mmol ZnO.

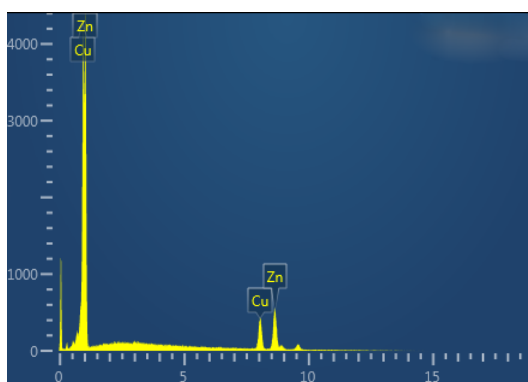


Figure 9. EDS spectrum of electrodeposits obtained at -2.05 V on a Cu cathode in the urea/EMIF (2:1 molar ratio) containing 3 mmol ZnO.

To identify the electrodeposits, some techniques were used. The XRD pattern of the electrodeposits is illustrated in the Figure 8. All peaks are indexed to Cu and Cu_5Zn_8 . 2θ values

(35.097, 38.013, 43.342, 62.965, 79.525, and 90.001) correspond to the main characteristic peaks of Cu_5Zn_8 crystals (reference code = 03-065-3157). It shows that the electrodeposit is Cu_5Zn_8 . Cu peaks are derived from the cathode. No other peaks are observed in this XRD pattern.

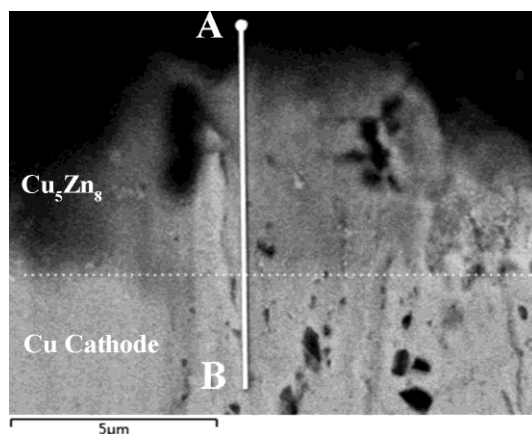


Figure 10. Cross-sectional SEM micrographs of electrodeposits obtained at -2.05 V on a Cu cathode in the Urea/EMIF (2:1 molar ratio) containing 3 mmol ZnO.

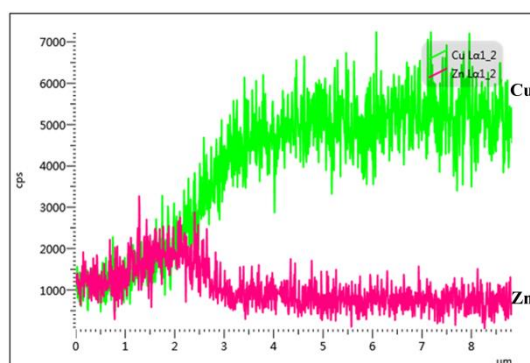
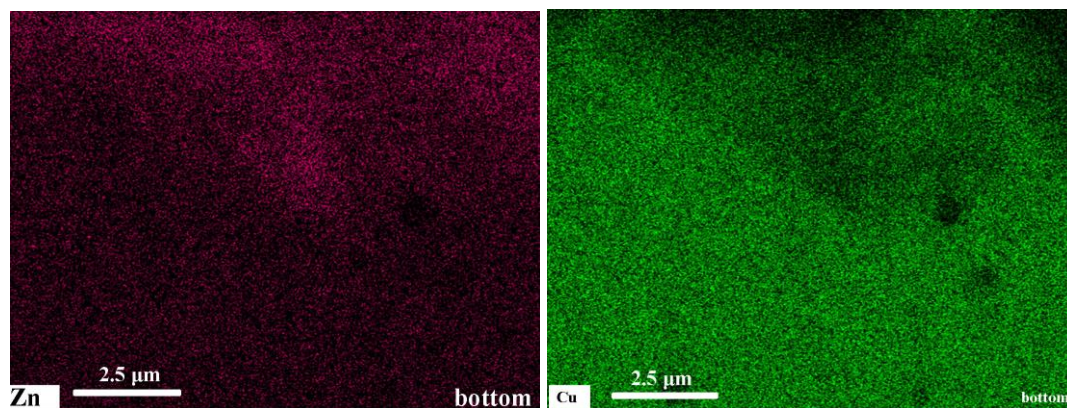


Figure 11. The distribution of Zn and Cu content obtained by EDS linear scanning from point A to B point in Figure 10.



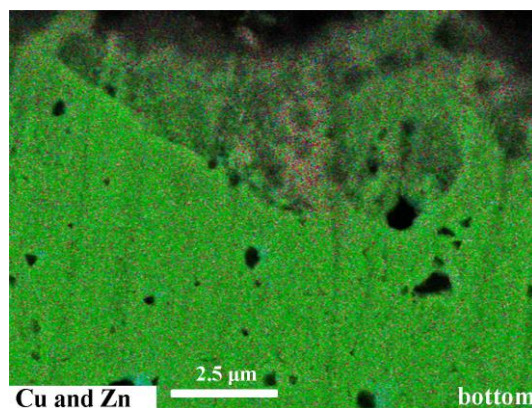
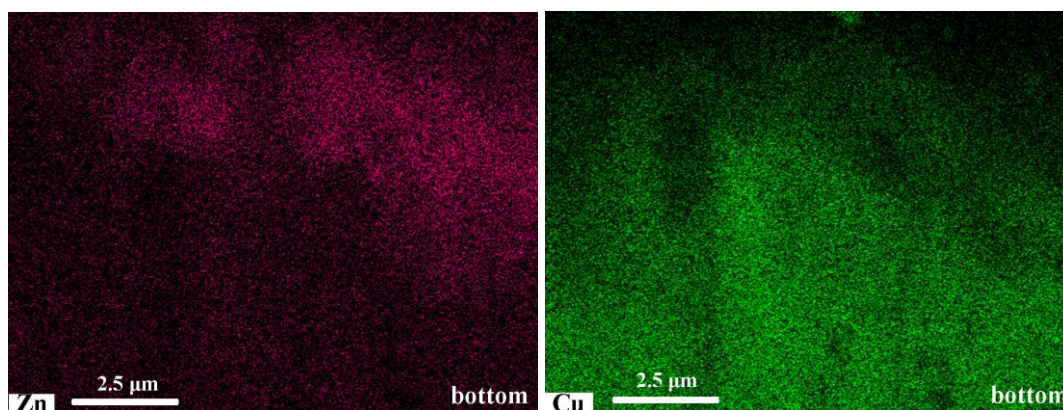


Figure 12. The distribution of Zn and Cu obtained by EDS area scanning for cross-sectional electrodeposits obtained at -1.90 V on a Cu cathode in the urea/EMIF (2:1 molar ratio) containing 3 mmol ZnO.

The EDS spectrum of electrodeposits is illustrated in Figure 9. Obviously, only Cu and Zn elements (Cu being derived from the cathode) are detected. And no other elements, such as F, N and O, are discovered on this spectrum, suggesting that the electrodeposit is free of residual electrolyte. The electrodeposits obtained on the Cu cathode from the ZnO-urea/EMIF system are identified to Cu_5Zn_8 alloy, as confirmed by XRD and EDS.

To investigate the elemental distribution of Cu_5Zn_8 alloy, we examined a cross-sectional SEM for the electrodeposits obtained on a copper cathode at -2.05 V, as shown in Figure 10. A distinguishable layer was generated on the surface of the copper cathode, and a similar phenomenon was found in a previous study [20]. To study the elemental composition of this layer, we performed an EDS linear scanning analysis on the sample (from A to B point in Figure 10), as presented in Figure 11. The concentration of zinc decreased gradually and that of the copper atoms increased from the surface to the inner cathode. Beyond $2\text{ }\mu\text{m}$ in Figure 11, we observed a significant change in the zinc and copper concentrations, which correspond to the elemental distributions of zinc and copper in Figure 10. This probably indicates that the thickness of the Cu_5Zn_8 layer was up to approximately $2\text{ }\mu\text{m}$. Meanwhile, no clear phase boundary was found between the Cu_5Zn_8 layer and the copper cathode. This may be related to the interdiffusion of the zinc and copper atoms.



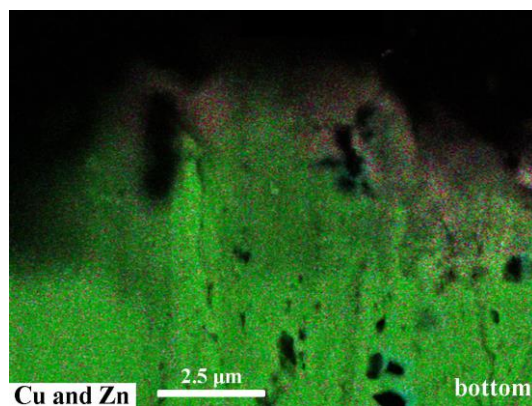


Figure 13. The distribution of Zn and Cu obtained by EDS area scanning for cross-sectional electrodeposits obtained at -2.05 V on a Cu cathode in the urea/EMIF (2:1 molar ratio) containing 3 mmol ZnO.

We performed cross-sectional EDS area scans for the samples deposited on the copper cathode at -1.90 V and -2.05 V, as shown in Figure 12 and 13, respectively. In both figures, we found that a high concentration of zinc atoms was distributed on the surface and the copper atoms were mainly concentrated at the bottom of the cathode. The interdiffusion between the zinc and copper atoms occurred and then generated Cu_5Zn_8 alloy, which has been confirmed by XRD. The concentration of zinc and copper atoms decreased gradually with increasing diffusion distance in the interdiffusion process. This may be related to the solid solubility limits. Compared with Figure 12, the zinc concentration in Figure 13 is higher on the surface. This may be due to the increased number of growth sites and increased electrodeposition rates at a more negative potential.

3.3 Formation mechanism of Cu_5Zn_8 alloy

Here, we propose a possible formation mechanism for Cu_5Zn_8 alloy, mainly comprising two steps: (1) the formation of zinc atoms; and (2) the interdiffusion between the zinc atoms and copper cathode.

(1) The formation of zinc atoms

When EMIF, urea and ZnO are mixed, hydrogen bonds formed between hydrogen, nitrogen, oxygen, and neighboring fluorine ions, which often cause a depression in the freezing point of the mixture [6, 12-14]. Urea plays a role of ligand agent in the ZnO-urea/EMIF system. It reacts with ZnO to form a complex, which delocalizes the charge and reduces the interaction between the anions and cations [6, 19]. Due to the strong influence of hydrogen bonds and the complex, the ZnO is facilitated to dissolve in the urea/EMIF. Then complexes containing zinc form in the electrolyte. Complexes containing zinc migrate to the Cu cathode and are reduced into zinc in the electrolysis process. Zinc nuclei are then generated and grow on the surface of the Cu cathode. Over long experimental times, zinc atoms are concentrated on the surface of Cu cathode.

(2) Interdiffusion between zinc atoms and copper cathode.

When many zinc atoms are deposited on the surface of a Cu cathode, a concentration gradient occurs on the interface between the zinc and copper atoms, which is liable to cause diffusion. This atom diffusion process includes both zinc to copper and copper to zinc. A similar observation had been reported regarding Cu-Zn alloy in a previous literature [2, 16]. From the surface to the inner cathode, as shown in Figs. 12 and 13, a distribution of the zinc atoms was sparser while that for copper atoms dispersed more and more dense. There is no obvious two-phase boundary between zinc and copper, as has also been observed in a previous study [20]. This indicates that interdiffusion does occur between the zinc and copper atoms. When enough zinc atoms and a sufficient diffusion time are supplied, Cu_5Zn_8 alloy is facilitated to form on the interface. Thermodynamically, a low Gibbs formation energy ($-161.15 \text{ kJ mol}^{-1}$ at 353 K) is required to generate Cu_5Zn_8 . This may suggest that Cu_5Zn_8 is thermodynamically stable at this temperature [15]. As shown in Figure 10, in the initial stage, the amount of Cu_5Zn_8 increases significantly and an obvious Cu_5Zn_8 layer was formed. The thickness of Cu_5Zn_8 was about $2.0 \mu\text{m}$. However, beyond $2.5 \mu\text{m}$, the thickness did not increase. And the zinc content drops quickly while that of coppers rises, as shown in Figure 11. This may be related to the solid solubility limits and to the fact that a thick Cu_5Zn_8 layer was formed on the interface hinders further interdiffusion between the zinc and copper atoms [3, 15, 21]. The formation process of Cu_5Zn_8 alloy is illustrated in Figure 14.

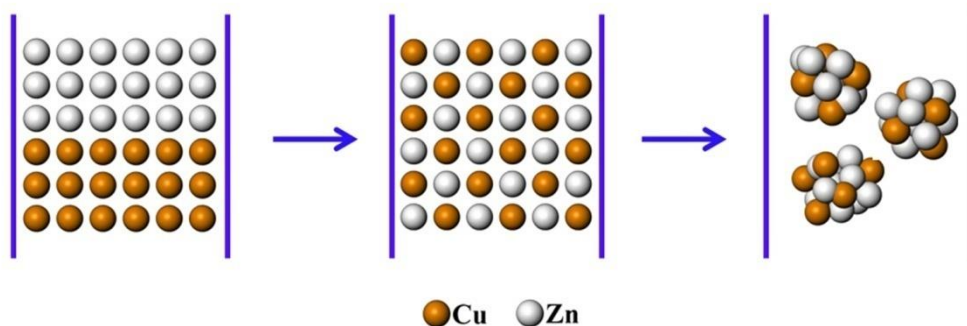


Figure 14. The process of forming Cu_5Zn_8 alloy on the interface between zinc and a Cu cathode in the urea/EMIF (2:1 molar ratio) containing 3 mmol ZnO.

4. CONCLUSIONS

In conventional methods, Cu_5Zn_8 alloy was prepared in extreme conditions required high temperatures, extreme pressures and huge currents. To be environmentally friendly, it's necessary to develop low-temperature and low-energy technology. In this study, a low temperature method for preparation of Cu_5Zn_8 alloy is performed electrochemically on a Cu substrate in ZnO-urea/EMIF system at 353 K. A new electrolyte, Urea/EMIF, is able to surprisingly dissolve zinc oxides. ZnO was chose as a zinc source and a Cu cathode was employed as the copper source in situ operation. The electrochemical behavior of zinc in ZnO-urea/EMIF system was investigated using chronoamperometric and cyclic voltammetric techniques. The results illustrated that the zinc reduction in the ZnO-urea/EMIF system is a diffusion-controlled irreversible process via a single-step two-electron transfer procedure. The diffusion coefficient was $7.4 \times 10^{-10} \text{ cm}^2 \text{ s}^{-1}$. Electrode reaction

becomes more reversible and equal potentials shift toward the positive direction as temperature increases from 333 to 373 K. Potentiostatic experiments are performed a Cu cathode and Electrodeposits are identified as Cu₅Zn₈ alloy, verified by XRD and EDS. The results of the EDS linear scanning analysis for electrodeposits showed that the thickness of the Cu₅Zn₈ layer was approximately 2 µm. The cross-sectional SEM presented that a high concentration of zinc atoms was distributed on the surface of cathode while the copper atoms were mainly concentrated on the bottom. A possible formation mechanism for Cu₅Zn₈ alloy was proposed, which mainly comprises two steps: (1) the formation of zinc atoms; and (2) the interdiffusion between the zinc atoms and copper cathode.

ACKNOWLEDGEMENTS

The authors would like to acknowledge the financial support from the National Natural Science Foundation of China (No. 51322406, 51474060 and 51574071); the Program for New Century Excellent Talents in University (NCET-2013-0107), Ministry of Education of China and the Fundamental Research Funds for the Central Universities (N140205001&L1502014).

References

1. U. Mizutani, T. Takeuchi and H. Sato, *Prog. Mater. Sci.*, 49 (2004) 227.
2. M. Farbod, A. Mohammadian, K. Ranjbar and R.K. Asl, *Metall. Mater. Trans. A*, 47 (2016) 1409.
3. Q. Wang, H. Yang, J. Shi and G. Zou, *Mater. Sci. Eng. A*, 307 (2001) 190.
4. M. Farbod and A. Mohammadian, *Intermetallics*, 45 (2014) 1.
5. N.K. Mukhopadhyay, D. Mukherjee, S. Bera, I. Manna and R. Manna, *Metall. Mater. Trans. A*, 485 (2008) 673.
6. F. Endres, D. MacFarlane, A. Abbott, *Electrodeposition from ionic liquids*, WILEY-VCH Verlag GmbH & Co. KGaA, (2008) Weinheim, Germany.
7. S. Ibrahim, A. Bakkar, E. Ahmed and A. Selim, *Electrochim. Acta*, 191 (2016) 724.
8. M.A. Miller, J.S. Wainright and R.F. Savinell, *J. Electrochem. Soc.*, 163 (2016) A578.
9. J. Zhang, M. An, Q. Chen, A. Liu, X. Jiang, S. Ji, Y. Lian and X. Wen, *Electrochim. Acta*, 190 (2016) 1066.
10. R. Maizi, P. Fricoteaux, A. Mohamadou, A. Meddour, C. Rousse, *Int. J. Electrochem. Sci.*, 11 (2016) 7111.
11. Y. Zheng, C. Peng, Y. Zheng, D. Tian, Y. Zuo, *Int. J. Electrochem. Sci.*, 11 (2016) 6095.
12. T. Sato, T. Maruo, S. Marukane and K. Takagi, *J. Power Sources*, 138 (2004) 253.
13. H. Sakaebe and H. Matsumoto, *Electrochem. Commun.*, 5 (2003) 594.
14. P.C. Howlett, D.R. MacFarlane and A.F. Hollenkamp, *Electrochem. Solid-State Lett.* 7 (2004) A97.
15. A. Kitada, K. Yanase, T. Ichii, H. Sugimura and K. Murase, *J. Electrochem. Soc.*, 160 (2013) D417.
16. Y.W. Lin, C.C. Tai and I.W. Sun, *J. Electrochem. Soc.*, 154 (2007) D316.
17. P.Y. Chen and I.W. Sun, *Electrochim. Acta*, 45 (2000) 3163.
18. J.S. Wilkes, J.A. Levisky, R.A. Wilson and C.L. Hussey, *Inorg. Chem.*, 21 (1982) 1623.
19. H. Yang, R.G. Reddy, *Electrochim. Acta*, 147 (2014) 513.
20. Y.C. Liu, J.B. Wan and Z.M. Gao, *J. Alloys Compd.*, 465 (2008) 205.
21. M.L. Huang, Q. Zhou, N. Zhao and Z.J. Zhang, *J. Electron. Mater.*, 42 (2013) 2975.
22. T.S.S. Dikshith, *Hazardous chemicals safety management and global regulations*, CRC Press Taylor & Francis Group, (2012) Boca Raton, USA.

23. A.J. Bard, L.R. Faulkner, *Electrochemical methods: fundamentals and applications*, 2nd Edition, *John Wiley & Sons*, (2001) New York, USA.
24. Derek Pletcher, *A first course in electrode processes*, 2nd edition, *The Royal Society of Chemistry*, (2009) London, UK.
25. H. Yang and R.G. Reddy, *Electrochim. Acta*, 178 (2015) 617.
26. W.R. Pitner and C.L. Hussey, *J. Electrochem. Soc.*, 144 (1997) 3095.

© 2017 The Authors. Published by ESG (www.electrochemsci.org). This article is an open access article distributed under the terms and conditions of the Creative Commons Attribution license (<http://creativecommons.org/licenses/by/4.0/>).